NOD.c3c4 congenic mice develop autoimmune biliary disease that serologically and pathogenetically models human primary biliary cirrhosis

Junichiro Irie,[1] Yuehong Wu,[1] Linda S. Wicker,[3] Daniel Rainbow,[3] Michael A. Nalesnik,[2] Raphael Hirsch,[4] Laurence B. Peterson,[5] Patrick S.C. Leung,[6] Chunmei Cheng,[6] Ian R. Mackay,[7] M. Eric Gershwin,[6] and William M. Ridgway[1]

[1]Division of Rheumatology and Immunology, and [2]Division of Pathology, University of Pittsburgh School of Medicine, Pittsburgh, PA 15261
[3]Juvenile Diabetes Research Foundation/Wellcome Trust Diabetes and Inflammation Laboratory, Department of Medical Genetics, Cambridge Institute for Medical Research, University of Cambridge, Cambridge CB2 2XY, UK
[4]Division of Rheumatology, Children's Hospital, Pittsburgh, PA 15213
[5]Department of Pharmacology, Merck Research Laboratory, Rahway, NJ 07065
[6]Division of Rheumatology and Clinical Immunology, School of Medicine, University of California, Davis, Davis, CA 95616
[7]Department of Biochemistry and Molecular Biology, Monash University, 3800 Victoria, Australia

Primary biliary cirrhosis (PBC) is an autoimmune disease with a strong genetic component characterized by biliary ductular inflammation with eventual liver cirrhosis. The serologic hallmark of PBC is antimitochondrial antibodies that react with the pyruvate dehydrogenase complex, targeting the inner lipoyl domain of the E2 subunit (anti–PDC–E2). Herein we demonstrate that NOD.c3c4 mice congenically derived from the nonobese diabetic strain develop an autoimmune biliary disease (ABD) that models human PBC. NOD.c3c4 (at 9–10 wk, before significant biliary pathology) develop antibodies to PDC–E2 that are specific for the inner lipoyl domain. Affected areas of biliary epithelium are infiltrated with CD3^{+}, CD4^{+}, and CD8^{+} T cells, and treatment of NOD.c3c4 mice with monoclonal antibody to CD3 protects from ABD. Furthermore, NOD.c3c4–scid mice develop disease after adoptive transfer of splenocytes or CD4^{+} T cells, demonstrating a central role for T cells in pathogenesis. Histological analysis reveals destructive cholangitis, granuloma formation, and eosinophilic infiltration as seen in PBC, although, unlike PBC, the extrahepatic biliary ducts are also affected. Using a congenic mapping approach, we define the first ABD (Abd) locus, Abd1. These results identify the NOD.c3c4 mouse as the first spontaneous mouse model of PBC.

CORRESPONDENCE
William M. Ridgway:
ridgway2@pitt.edu

Abbreviations used: ABD, autoimmune biliary disease; ANA, antinuclear antibody; CBD, common bile duct; CBDD, CBD dilation; HLC, hepatic lymphoid cell; Idd, insulin-dependent diabetes; NOD, nonobese diabetic; NSDC, nonsuppurative destructive cholangitis; PBC, primary biliary cirrhosis; PDC, pyruvate dehydrogenase complex.

Primary biliary cirrhosis (PBC) is an autoimmune liver disease of middle-aged women characterized by a progressive portal lymphocytic inflammatory response and destruction of intrahepatic bile duct epithelial cells. A serologic hallmark of PBC is autoantibodies reactive with the mitochondrial subunits of the 2-oxoacid dehydrogenase complexes, particularly the E2 subunit of the pyruvate dehydrogenase complex (PDC–E2), which appear long before the clinical onset of disease (1–3). The epitopes recognized by anti–PDC–E2 and autoreactive CD4^{+} and CD8^{+} T cells map within the inner lipoyl domain of PDC–E2 (4–6).

Intriguingly, the mitochondrial PDC–E2 auto-antigen is found in all nucleated cells in the body, yet the bile duct epithelial cells in which mitochondria are relatively sparse are the major target of immunodestruction. An understanding of how a ubiquitous self-antigen, PDC–E2, becomes a focus of autoimmune reactivity, with damage only in the biliary system, is central to understanding the pathogenesis of PBC. Hitherto, the lack of an animal model has been a major handicap, leading to reliance on small liver biopsy samples and explant livers in the advanced stages of disease to define the immunological status of the portal triad.

Recently, we reported that the NOD.c3c4 mouse, which is completely protected from diabetes by B6/B10 regions on chromosomes 3 and 4 that contain B6/B10 insulin-dependent diabetes (*Idd*) loci, spontaneously developed an autoimmune biliary ductular disease with lymphocytic infiltrates, antinuclear antibodies (ANAs), and eventually fatal biliary obstruction (7). The disease could be transferred by splenocytes to naive mice, suggesting an autoimmune etiology (7). The nonobese diabetic (NOD) mouse is well known as a model of autoimmune type 1 diabetes that results from a spontaneous T lymphocytic attack on pancreatic islet β cells (8). In addition, older NOD mice develop lymphocytic infiltrates at other sites, notably salivary and lacrimal glands, and the thyroid gland (9), but the liver is spared. Interestingly, NOD congenic mice bearing a non–NOD MHC region develop a Sjogren's-like syndrome (10), and a TCR transgene on the NOD background results in a spontaneous articular disease closely resembling rheumatoid arthritis (11). Collectively, NOD and genetically modified NOD mice (NOD congenics and NOD transgenics) represent a remarkable kindred of genetically related mice that express the same types of diseases seen in kindreds of patients with PBC, particularly type 1 diabetes, rheumatoid arthritis, Sjogren's syndrome, and thyroiditis.

We report herein several components of disease shared between the NOD.c3c4 and PBC, narrow the genetic intervals necessary for disease, and define the first autoimmune biliary disease (ABD)–associated locus (*Abd1*). Our data demonstrate that NOD.c3c4 mice have CD3^{+}, CD4^{+}, and CD8^{+}

T cell infiltrates in affected biliary epithelium. The CD4^{+} fraction of the NOD.c3c4 cell population produces multiple cytokines, and the hepatic lymphoid cell (HLC) population changes over the course of disease. Anti-CD3 treatment prevents disease onset and NOD.c3c4-*scid* mice develop ABD after the adoptive transfer of T cells from diseased NOD.c3c4 mice, demonstrating a pathologic role for T cells in the disease process. Finally, NOD.c3c4 mice spontaneously develop autoantibodies to PDC-E2 as early as day 67, well before the appearance of ANAs and other autoantibodies previously described in NOD mice (7). Collectively, these findings demonstrate coordinate dysregulation of both T and B cell responses to biliary tissue in this model, establishing this as a spontaneous mouse model of PBC.

RESULTS
Genetic dissection of ABD defines a disease causative region (*Abd1*) on chromosome 4

NOD.c3c4 mice have large chromosome 3 and chromosome 4 B6/B10-derived regions of the genome introgressed onto the NOD background. Each is ∼80 megabases (Fig. 1). As we reported previously, strain 1802 develops ABD, although with reduced penetrance (7). Strain 1802 has the same B10 chromosome 4 interval as NOD.c3c4, but a significantly decreased chromosome 3 interval, eliminating the large region of introgressed B6-derived DNA between *Idd3* and *Idd10/18*, including the *Idd17* region (Fig. 1). We dissected the genetic regions on chromosome 4 necessary for disease. The 1803 mouse was constructed with the same interval on chromosome 3 as strain
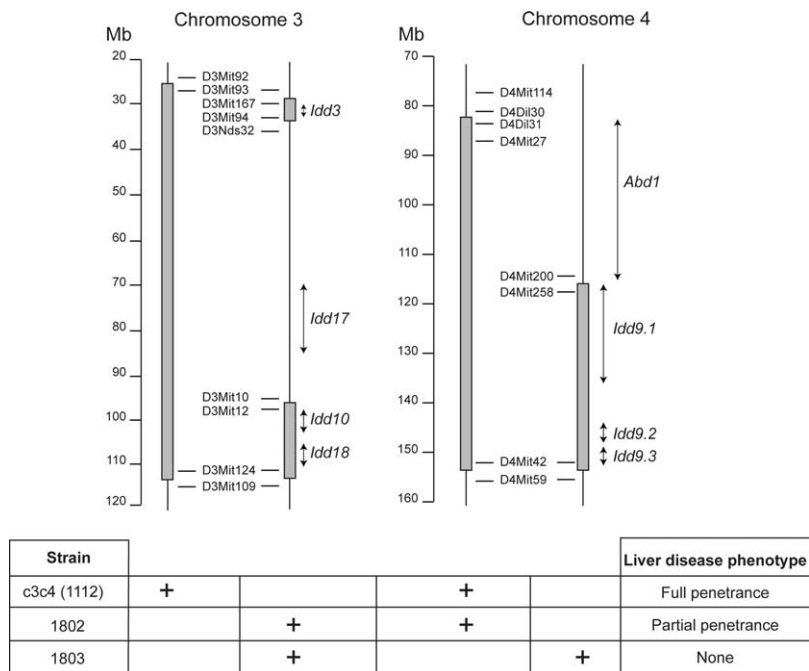

Figure 1.   Genetic map of NOD.c3c4, 1803, and 1802 defining *Abd1*. Strain 1802 develops biliary disease, although at decreased penetrance compared with NOD.c3c4. Strain 1803 is free from ABD and differs from 1802 only on the upper portion of the chromosome 4 segment (labeled *Abd1*), which is distinct from the known chromosome 4 *Idd* regions.
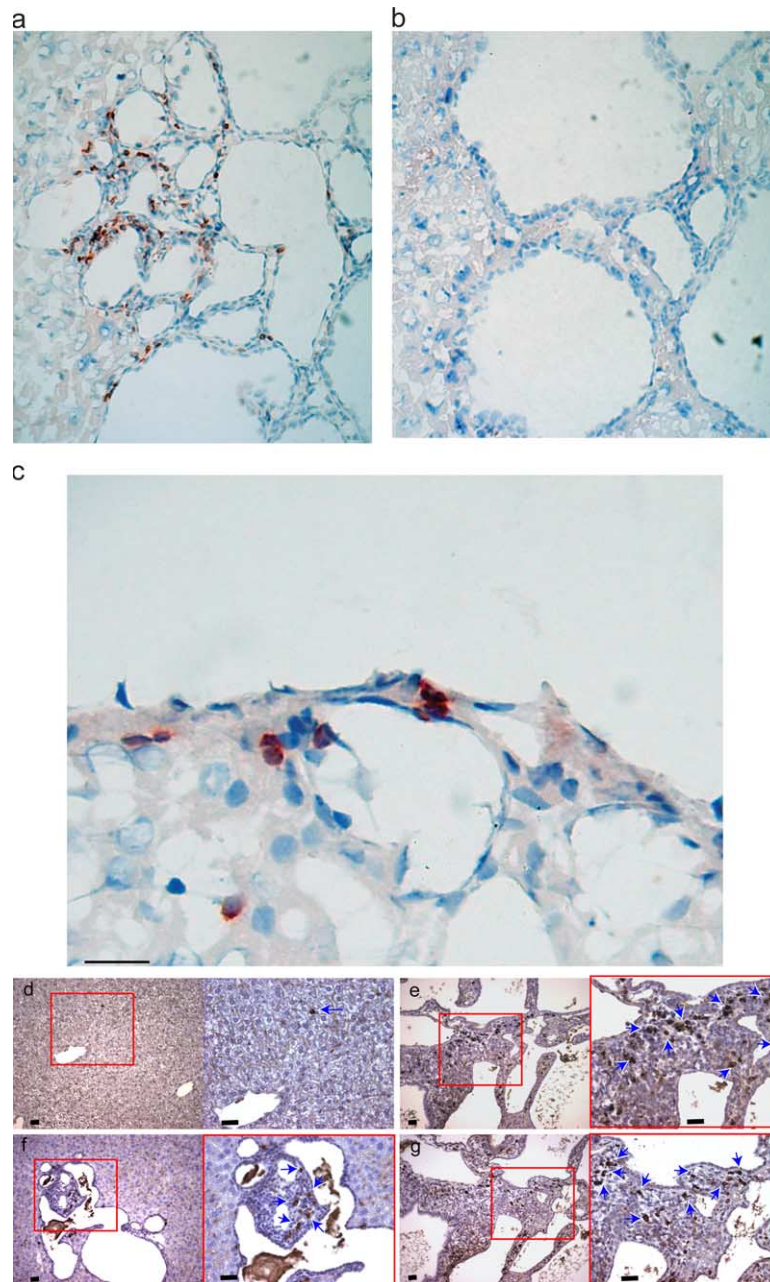
Strain					Liver disease phenotype
c3c4 (1112)	+			+	Full penetrance
1802		+		+	Partial penetrance
1803		+			+	None

Figure 2. Invasion by CD3+, CD4+, and CD8+ cells of NOD.c3c4 biliary epithelium. Immunohistochemistry using anti-CD3 (a) or isotype control antibody (b) on NOD.c3c4 liver sections, showing CD3+ cells (reddish-brown) directly adjacent to biliary epithelial cells in areas of cyst formation, but not adjacent to hepatocytes. (c) Magnified view showing CD3+ cells located directly adjacent to biliary epithelial cells (blue). (d) Control B6 liver showing lack of lymphocytic infiltrates, (e) immunohistochemical staining of CD4+ T cells infiltrating the peribiliary region, adjacent to cystic biliary changes, and (f) immuno-histology of CD8+ mononuclear lymphoid cells in NOD.c3c4 mice. Note the presence of aggregated as well as dispersed CD8+ mononuclear cells (arrows) infiltrating the portal tracts. (g) Immunohistochemical staining of pDCA1+ dendritic cells in the peribiliary infiltrate. All bars, 50 μm.

1802, but with a truncated interval on chromosome 4 (Fig. 1). Notably, strain 1803 retained the known chromosome 4 *Idd* loci *1dd9.1*, *9.2*, and *9.3*, but was completely protected from ABD because none of 16 mice aged up to 50 wk had liver disease. These data define an ∼30-megabase region of chromosome 4, which is both necessary for ABD and separate from the *Idd* loci necessary for autoimmune diabetes. Therefore, we have defined the first ABD-specific locus (*Abd1*; Fig. 1).

Comparable liver histology in NOD.c3c4 mice and PBC

We previously identified lymphocytic infiltrates around biliary epithelium in 44% of 8-wk-old and 71% of 16-wk-old
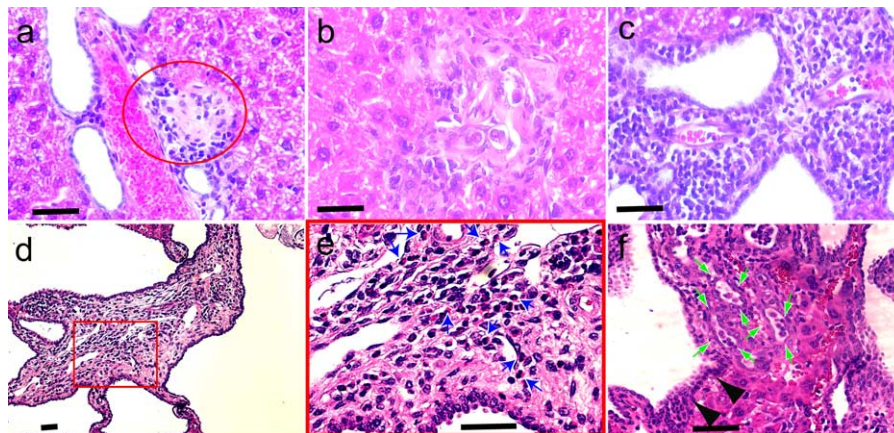
Figure 3. Histological sections of (a–c) 20– and (d–f) 30–wk–old NOD.c3c4 mice livers showing lesions comparable to PBC. (a) Granulomatous lesion in a portal area, (b) chronic NSDC in portal area, and (c) peribiliary lymphoplasmacytic infiltration. Progression of the liver pathology in 30-wk-old NOD.c3c4 mice is shown by (d) pronounced biliary polycystic changes with infiltration of inflammatory cells, (e) fibrosis in the portal areas with eosinophilic infiltration (blue arrows), (f) hyperplasia of biliary epithelium with dilation of bile duct (black arrows) and degenerative biliary ductules with macrophage aggregates in the lumen (green arrows). All bars, 50 μm.

NOD.c3c4 mice (7). Using immunohistochemistry, we identified these as predominantly CD3$^+$ T cell infiltrates. These infiltrates were not adjacent to hepatocytes (Fig. 2, a and b), but rather adjacent to biliary epithelial cells (Fig. 2 c), consistent with direct interaction of T cells with biliary epithelial cells. Further immunohistochemical analysis demonstrated that the peribiliary CD3$^+$ cells were comprised of cells from CD4$^+$ and CD8$^+$ lineages (Fig. 2, e and f). Moreover, NOD.c3c4 peribiliary regions, but not those of control strains, demonstrated infiltrating pDCA1$^+$ dendritic cells (Fig. 2 g).

Human PBC is histologically characterized by early periductular granuloma formation as well as portal eosinophilic infiltrates and destruction of small hepatic ducts, called nonsuppurative destructive cholangitis (NSDC; references 12–14). Terasaki et al. (13) found that earlier eosinophilic infiltration correlated positively with peribiliary lymphoid infiltrates, granuloma formation, and duct lesions. Later stages are marked by fibrosis and eventual cirrhosis. In this study, we confirmed our previous findings of anatomical abnormalities consisting of marked biliary polycystic disease in the liver in almost all 20–30-wk-old NOD.c3c4 mice (7) but have identified novel histological findings comparable to human PBC. Histologically, biliary cyst formations were found in the intrahepatic biliary tree, whereas bile duct damage including NSDC-like lesions was identified, primarily in the small intrahepatic bile ducts (Fig. 3). Specifically, peribiliary lymphocytic infiltration and interlobular bile duct damage including NSDC-like lesions with macrophage aggregates in the lumen were found in seven out of seven NOD.c3c4 mice, eosinophilic infiltration and early fibrosis were found in two out of seven NOD.c3c4 mice, and epitheloid granuloma–like lesions were found in one out of seven NOD.c3c4 mice (Fig. 3, a–f). In older mice (30 wk), biliary polycystic changes became more prominent and may even mask the NSDC-like lesion.

We further analyzed the HLC population in NOD.c3c4 mice by comparison with that of biliary disease-free NOD, 1803, and B6.G7 mice. The composition of the HLC populations differed markedly from that of spleen or lymph nodes due to an increased percentage of NK, γ-δ T cells, and NKT cells, although the proportions of cell subsets in pre-disease NOD. c3c4, NOD, and 1803 mice were comparable (Fig. 4 a). However, the HLC composition changed in NOD.c3c4 mice compared with disease-free 1803 mice and young NOD mice (Fig. 4 b). NOD.c3c4 mice developed an increased number of granulocytes (Fig. 4 b) and a decrease in the CD4/CD8 ratio from 5 in pre-disease mice to 2 after 30 wk of age (not depicted).

Cytokine production by HLCs in NOD.c3c4 mice

To further characterize the HLCs from NOD.c3c4, we measured cytokine production and compared this with production by lymph node or splenic cells from the same animal (Fig. 5). Ribonuclease protection analysis demonstrated considerable production of IL-4, IL-5, IL-10, and IL-13 mRNA only in stimulated NOD.c3c4 HLC CD4$^+$ cells and not in peripheral CD4$^+$ lymph node cells from the same animal (Fig. 5 a). HLCs stimulated with anti-CD3 and anti-CD28 demonstrated abundant IL-4 protein production, whereas lymph node and splenic cells from the same animal produced none (Fig. 5 b). To further characterize the cellular source of HLC cytokine production, we fractionated the total HLC population into CD4$^+$ and CD8$^+$ populations and assayed cytokine production by each after stimulation with anti-CD3 and anti-CD28 mAbs (Fig. 5 c). CD4$^+$ T cells in the HLC population were clearly the source of almost all IFN-γ and IL-2 production (Fig. 5 c).

Anti–CD3 treatment ameliorates disease course in NOD.c3c4 mice

The presence in NOD.c3c4 mice of CD3$^+$, CD4$^+$, and CD8$^+$ T cells infiltrating the biliary epithelium, together
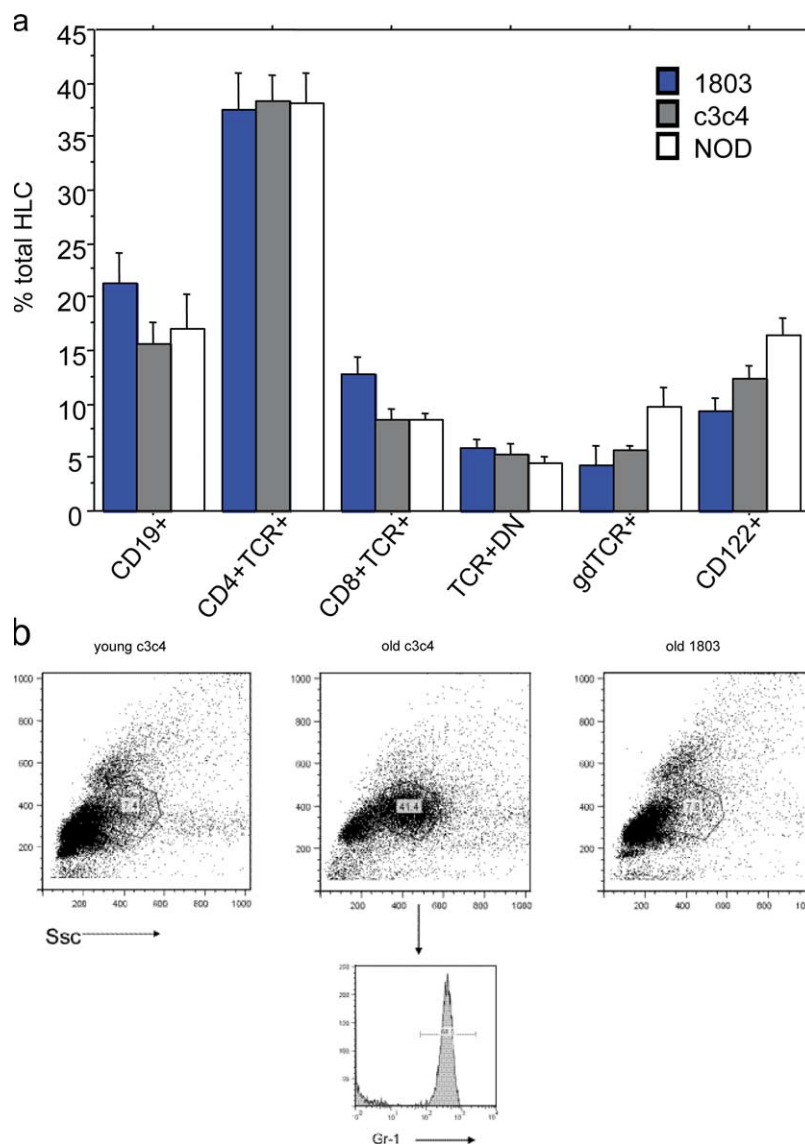
Figure 4. Cellular composition of the HLC population changes with age in NOD.c3c4, but not strain 1803, mice. (a) The NOD.c3c4 HLC population does not differ from that of NOD or 1803 mice before 30 wk of age. HLCs were isolated, stained with surface markers, lymphocyte gated, and analyzed by FACS (see Materials and methods) from NOD, 1803, and NOD.c3c4 mice. There was no significant difference in cell composition between NOD, NOD.c3c4, or 1803 mice (1803 NOD, n = 3–5; NOD.c3c4, n = 8–10, except in the case of $\gamma\delta$T; NOD.c3c4, n = 4). All mice were 15–25 wk old. (b) Granulocyte accumulation in aged NOD.c3c4 mice. In NOD.c3c4 and 1803 >30 wk old, HLCs were isolated and analyzed by FACS as described above, using granulocyte gates (circled areas). Aged NOD.c3c4 showed a significantly increased accumulation of GR-1^{+} cells (41.4%) compared with aged 1803 mice (7.8%), which did not differ from young NOD.c3c4 mice (7.4%).

with active cytokine production by CD4^{+} HLCs, suggested a critical role for CD3^{+} T cells in pathogenesis. We sought to confirm this by T cell–directed immunotherapy because anti-CD3 antibodies prevent type 1 diabetes in NOD mice (15). A single injection of 200 μg anti-CD3 ameliorated disease in NOD.c3c4 mice. 3 out of 12 anti-CD3–treated NOD.c3c4 mice developed ABD compared with 6 out of 8 PBS-treated mice (P = 0.028). Anti-CD3 treatment was associated with a persistent, significant (P = 0.04) decrease in the number of HLC CD69^{+} T cells (Fig. 6). The decreased number of CD69^{+} cells was specific to the HLC population,

as splenic populations did not differ between treated and control mice (Fig. 6).

Early involvement of the common bile duct (CBD): a specific predictor of disease

We obtained an additional clue to the pathogenesis of ABD by the surprising discovery in young NOD.c3c4 mice of involvement of the CBD illustrated by comparison of the caliber of the CBD and portal vein. The ratio is ∼1:1 in normal mice but considerably greater in NOD.c3c4 mice (Fig. 7). This unique dilation of the CBD was found in very young mice.
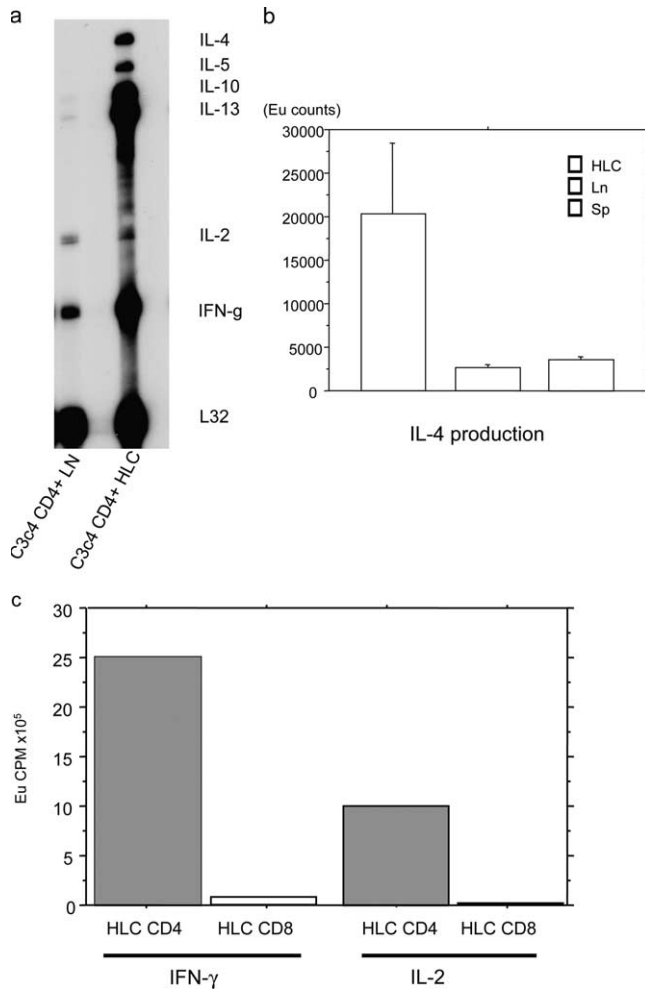
Figure 5. Differential cytokine production from HLCs and peripheral tissue lymphoid cells. (a) CD4+ cells were isolated from HLCs or peripheral lymphoid tissue (lymph node, spleen) and stimulated with anti-CD3/CD28 for 3 d before ribonuclease protection assay (see Materials and methods). Only HLC CD4+ T cells produced detectable amounts of IL-4, IL-5, IL-10, or IL-13. Data are representative of four separate experiments. (b) HLCs or peripheral lymphoid cells were stimulated for 3 d, and supernatants were collected and assayed for IL-4 production (see Materials and methods). Only HLCs produced substantial amounts of IL-4. The mean + SEM for multiple experiments is shown (LN and HLC, $n = 4$ experiments; spleen, $n = 2$). (c) CD4+ cells are the source of HLC cytokines. NOD.c3c4 HLCs were isolated as described above, purified into CD4+ and CD8+ cell fractions, and stimulated for 3 d, with anti-CD3/CD28 and supernatants collected for ELISA. Only the CD4+ fraction produced measurable amounts of IL-2 or IFN-γ. Data are representative of four separate experiments.

70% of NOD.c3c4 had CBD dilation (CBDD) at 3 wk of age, a pathology never seen in NOD, B6.G7, 1803, or any other mouse that did not develop ABD. We examined 40 NOD.c3c4 mice aged 24 wk and less. 18 out of 24 female and 11 out of 16 male mice in this age range demonstrated CBDD. To determine whether this finding had predictive power for disease, we examined 20 NOD.c3c4 mice aged >30 wk and 16 had CBDD. Histologically, there was a 100%

correlation for all 16 mice between CBDD and histological evidence of ABD, suggesting that the extrahepatic bile duct lesion is an essential component in the autoimmune process. Histological examination of the CBD confirmed pathological involvement, and, exclusively, NOD.c3c4 mice demonstrated thickening of the wall of the CBD, tortuous dilation, and a substantial subepithelial lymphocytic infiltrate (Fig. 7 a). Notably, anti–CD3 treatment prevented these changes (Fig. 7 b).

Transfer studies further define disease pathogenesis
The finding that CBDD is an early and highly specific marker of disease activity prompted us to perform transfer studies using CBDD as a disease phenotype that can be assessed more quickly than histology. We demonstrated previously that we could use irradiated NOD.c3c4 mice as transfer recipients (7). We used our newly constructed, disease-resistant 1803 strain to test if *Abd1* on hematopoietic donor cells alone was sufficient to transfer disease. We also used NOD.*scid* recipients to avoid irradiating the recipient mice and to test if disease could be transferred to a strain lacking the B6/B10 disease–associated regions. We transferred 20×10^6 whole splenocytes from diseased NOD.c3c4 female donors into a total of five female 1803, six female NOD-*scid*, and four positive control–irradiated female NOD.c3c4 recipients as described previously (7) and assessed CBDD between 5 and 14 wk after transfer. Consistent with our previous report, four out of four NOD.c3c4 recipients developed disease. Two of the mice studied developed CBDD at 5 wk after transfer. In contrast, none of the six NOD.*scid* recipients and none of the five 1803 recipients developed CBDD, remaining disease free even 3 mo after transfer. Because the 1803 strain lacks a B10 allele at the *Abd1* region compared with NOD.c3c4, these results demonstrate that *Abd1* expression in the recipient is required to induce ABD when splenocytes are transferred from diseased donors.

Using irradiated recipients is not ideal because radiation alone has a disease-modifying effect (7) and may alter the biology of the recipient mouse. To circumvent this problem and allow detailed analysis of ABD pathogenesis, we developed a NOD.c3c4-*scid* strain and performed transfer studies as outlined above. None of the four NOD.c3c4-*scid* mice receiving PBS alone developed CBDD at 4 wk after transfer, whereas three out of three NOD.c3c4-*scid* recipients receiving 20×10^6 splenocytes from diseased NOD. c3c4 donors developed CBDD. These results confirm the role of the hematopoietic system in disease pathogenesis. Moreover, they demonstrate that if *Abd1* is expressed in the recipient, even in the absence of functioning lymphocytes, hematopoietic cells from donors with ABD can transfer disease. Finally, to further narrow the subset of cells transferring disease, we purified CD4+ cells from diseased NOD.c3c4 splenocytes and transferred 14×10^6 CD4+ cells into NOD.c3c4-*scid* and NOD-*scid* recipients. At 4 wk after transfer, two out of three NOD.c3c4-*scid* recipients developed CBDD, whereas none of the three NOD-*scid* recipients showed CBDD. These results demonstrate that
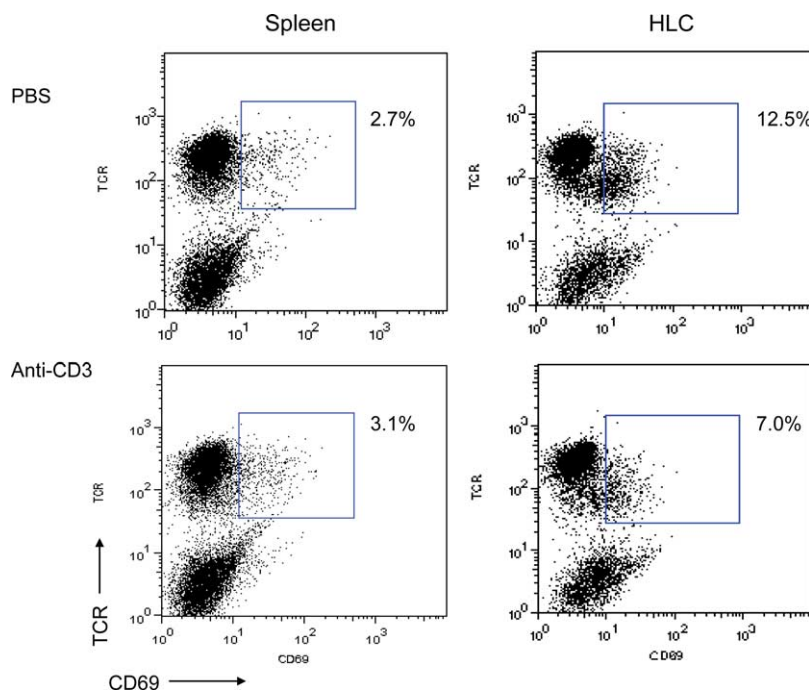
Figure 6. Anti–CD3 treatment of NOD.c3c4 mice ameliorates ABD and decreases the number of TCR⁺ CD69⁺ cells in the HLC population. Mice were treated with either a single dose of 200 μg anti-CD3 antibody in PBS or PBS alone between 6–10 wk of age, and HLC TCR⁺CD69⁺ cells were quantitated at ∼12 wk after treatment. A single dose of anti-CD3 antibody significantly reduced the number of TCR⁺CD69⁺ cells in the HLCs, but not in the spleen, compared with PBS-treated animals. Data shown are one representative of three separate experiments.

CD4⁺ cells alone are sufficient to transfer ABD to a genetically susceptible host.

NOD.c3c4 mice, in contrast to NOD, NOD.c3, or NOD.c4 mice, develop anti–PDC-E2 at an early age

We demonstrated previously that NOD.c3c4 and NOD.c4 mice developed autoantibodies, including ANA and anti-Sm (7). To test for autoantibodies characteristic of human ABD, we examined sera from NOD, NOD.c3, NOD.c4, and NOD.c3c4 mice for AMA. Negative tests were obtained for six out of six NOD female mice, six out of six NOD.c4 female mice, and six out of six NOD.c3 female mice. In contrast, a high proportion (10 out of 18) of female NOD.c3c4 mice produced anti–PDC-E2 (Fig. 8). Kinetic analysis of PDC-E2 reactivity revealed a markedly different pattern than that observed for ANA in NOD.c3c4 mice (Fig. 8 b). Serum samples from three out of five female NOD.c3c4 mice examined at 9–10 wk of age were ANA⁻ but had anti–PDC-E2 antibodies even though the mice did not yet have detectable liver lymphocytic infiltrates histologically. At later time points, four out of seven female NOD.c3c4 mice tested at 14–20 wk of age were anti–PDC-E2⁺, as were three out of six female mice tested at 20–25 wk of age. Although ANA positivity developed later and persisted in NOD.c3c4 mice, anti–PDC-E2 developed earlier, peaked, and declined in frequency with age (Fig. 8 b). To confirm the antigenic specificity of the anti-PDC antibodies, we used two approaches.

First, an enzymatic inhibition assay demonstrated that only human sera from PBC patients and NOD.c3c4 sera, not control sera, inhibited the enzymatic activity of PDC in a substrate-dependent manner (Table I). Second, use of recombinant proteins covering the major PDC-E2 domains, the inner and outer lipoyl domains, the E1/E3 binding site, and the catalytic domain showed that NOD.c3c4 sera were reactive only to the PDC-E2 inner lipoyl domain, which is the site of the dominant epitope for human PBC sera (Table II).

DISCUSSION

The NOD.c3c4 mouse expresses a spontaneous ABD that provides for the first time a model of human PBC. In this report, we demonstrate multiple immune abnormalities specific to the NOD.c3c4 mouse: CD3⁺, CD4⁺, and CD8⁺ T cells infiltrate the biliary epithelium in affected areas of the liver; CD4⁺ T cells produce excess cytokines; the composition of the HLC changes with age only in diseased NOD.c3c4 mice;

Table I. Inhibition of PDC enzyme activity by autoantibodies

Group	% Inhibition ± SEM
AMA⁺ c3c4 (n = 6)	54.73 ± 10.72ᵃ
NOD (n = 6)	5.3 ± 3.2
PBC (n = 6)	63.38 ± 8.74ᵃ
Control human	1.25 ± 0.85

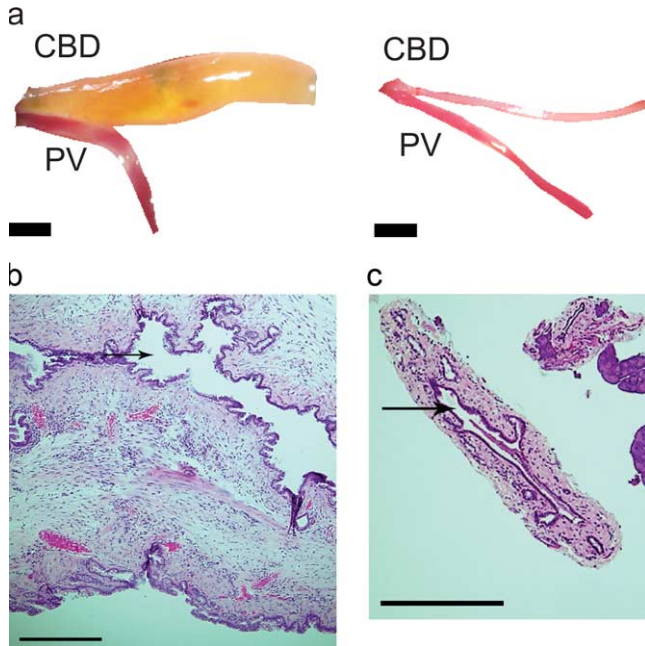ᵃP < 0.001 when compared with NOD and control human.

Figure 7. Dilated CBD is an early and specific indication of NOD.c3c4 biliary disease and reflects lymphocytic infiltration. (a) Substantially dilated CBDs (CBD) compared with the portal vein (PV) are found only in NOD.c3c4 mice (left) with liver disease, but not in NOD mice (right) or any other strains in absence of biliary disease. Bars, 1.5 mm. CBD and PV are shown digitally cropped from surrounding tissue. (b) Dilated NOD.c3c4 CBDs demonstrate lymphocytic infiltrates, tortuosity, and medial thickening (left). Anti-CD3 treatment (right) prevented histological abnormalities. Arrows point into the CBD lumen. Bars, 500 μm.

Figure 8. NOD.c3c4 mice develop anti–PDC-E2 antibodies at an early age. (a) Recombinant PDC-E2 was resolved by SDS-PAGE, transferred onto a nitrocellulose membrane, and probed with NOD.c3c4 sera (lanes 1 and 2); NOD.C3, NOD.C4, and NOD sera (lanes 3–5); and an mAb to PDC-E2 (lane 6), all at a 1:200 dilution. Reactivity was revealed by enhanced chemiluminescence (see Materials and methods). (b) Time course of NOD.c3c4 mice of anti–PDC-E2 and ANA reactivity from early age to 200 d. Significance according to Fisher's exact test.

and specific serum autoantibody to PDC-E2 is demonstrable at the relatively early age of 9–10 wk. Moreover, treatment with anti-CD3 antibody ameliorates expression of the disease and decreases the number of intrahepatic CD69^{+} T cells. Finally, CD4^{+} cells from diseased donors are sufficient to transfer disease into NOD.c3c4-*scid* mice. These findings demonstrate an essential role for T cells in the disease process. Genetic studies of the NOD.c3c4-related strain 1803 demonstrated that there is at least one locus specifically required for the development of ABD, which we have designated *Abd1* (Fig. 1). To have any penetrance of ABD, there must be a B10 allele at the *Abd1* locus in addition to B6 alleles at loci on chromosome 3 that overlap with regions known to influence susceptibility to type 1 diabetes: *Idd3*, *Idd10*, and *Idd18*. Transfer studies into the 1803 strain demonstrate that the presence of *Abd1* in the transferred hematopoietic cells is not sufficient to induce disease. The successful transfer of

Table II. Epitope mapping of anti–PDC-E2

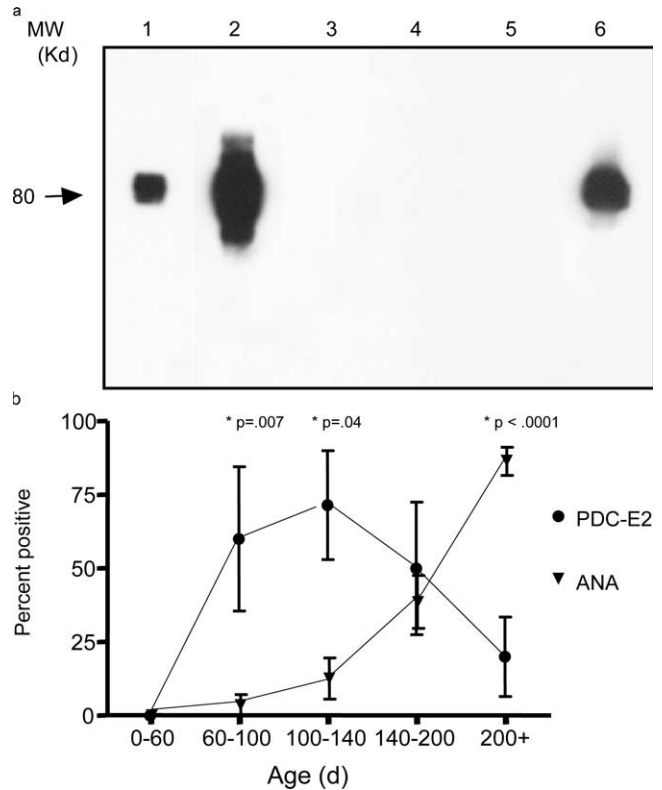| PDC-E2 domains	NOD.c3c4	NOD
Outer lipoyl	Negative	Negative
Inner lipoyl	Positive	Negative
E1/E3 binding site	Negative	Negative
Catalytic domain	Negative	Negative

ABD into NOD.c3c4-*scid* recipients requires *Abd1* to be expressed in at least some cells of the recipient.

We also describe a highly specific marker of disease that appears as early as 3 wk of age in NOD.c3c4 mice, but not in NOD, 1803, or any other mouse strain lacking ABD, namely CBDD, which correlated closely with histological disease. Microscopically, NOD.c3c4 mice show specific hepatic lesions in portal tracts analogous to those in human PBC, including epithelial granuloma-like formation, NSDC-like lesions, eosinophilic infiltrates, and early fibrosis. Moreover, with age, the liver of NOD.c3c4 mice has an increasing number of granulocytes as well as a decreased CD4/CD8 ratio, which is significant because in human PBC, myeloperoxidase^{+} cells may contribute to bile duct damage (16) and CD8^{+} cells are implicated in pathogenesis (17, 18). Finally, we demonstrate for the first time to our knowledge spontaneous development at a young age (9–10 wk) of autoantibodies to PDC-E2 in this mouse model. Such antibodies hitherto have been experimentally induced in mice but never observed to occur spontaneously (19). Similar to anti–PDC-E2 activity in PBC patients, sera from NOD.c3c4 mice

inhibited PDC enzyme function and reacted with an epitope within the inner lipoyl domain of PDC-E2. Anti–PDC-E2 preceded the detection of histological abnormalities in the liver as well as the development of ANA (7), equivalent to the occurrence of anti–PDC-E2 in patients several years before the overt onset of PBC.

The results presented here raise interesting questions. First, how closely does this model resemble human PBC? The strongest and likely most important resemblance is the spontaneous early occurrence of autoantibodies to PDC-E2 before the development of biliary ductular abnormalities. The overall prevalence of anti–PDC-E2 is less in NOD.c3c4 mice (56%) than in humans with PBC (90–95%). Moreover, some mice do develop histological ABD but not anti–PDC-E2. However, "AMA⁻ PBC" is well known in humans and can account for up to 10% of all patients with PBC. We also note that various mouse strains have different penetrance of genes for autoantibody production; i.e., the MRL/Mp-*lpr/lpr* mice develop anti-Sm antibodies at a 25% incidence in a manner that appeared genetically controlled but stochastic (20). We regard the spontaneous development of anti-PDC antibodies as critically important, despite the lack of full penetrance, for several reasons. One is that an understanding of the development of these antibodies that are so constantly associated with PBC should provide insights into the induction of the human counterpart, and may well dispel the longstanding concern that such antibodies are not truly disease relevant but rather are simply epiphenomena. Another is that the appearance of anti–PDC-E2 in NOD.c3c4 mice, even if not directly or indirectly contributing to disease, points to specific T cell help for their generation. This, together with our finding of CD3⁺, CD4⁺, and CD8⁺ T cell infiltration of the biliary epithelium, production by CD4⁺ T cells of the majority of the proinflammatory cytokines, amelioration of disease by anti-CD3, and transfer of disease by CD4⁺ cells into NOD. c3c4-*scid* mice, which are T and B cell deficient, indicates a major T cell response to PDC-E2 in these mice as in human PBC (1). Detailed dissection of the T cell epitope response to PDC-E2 in NOD.c3c4 mice is under active investigation in our laboratories. Another interesting aspect of disease in NOD.c3c4 mice is the role of sex in disease outcome. We originally reported earlier mortality in females compared with male mice, and that female mice had higher autoantibody titers (7). Here we have studied this issue in much more detail and report that male and female NOD.c3c4 mice develop CBDD, as well as histological evidence of disease that correlates very highly with CBDD, with equal prevalence. Moreover, male and female mice show statistically indistinguishable numbers of ANA⁺ mice until 200 d old, although female mice older than 200 d may show a trend to a higher prevalence of ANA positivity. We therefore cannot conclude that the increased mortality originally reported for female mice is due to a greater prevalence of autoimmunity in these mice; e.g., male mice may resist the autoimmune liver disease longer because of increased body weight or some other confounding factor.

This is an interesting issue that will require further studies to elucidate.

A disease feature by which NOD.c3c4 ABD differs from PBC is the site of the initial autoimmune attack, the CBD versus intrahepatic cholangiocytes. Virtually all mice with ABD initially develop an abnormally dilated CBD characterized histologically by lymphocytic infiltration, a feature lacking in the pathology of PBC. Still, it is intriguing that this initial lesion results from an immune response occurring at the gut: CBD interface. The small intestine, pancreatic duct, and CBD constitute an "anatomic nexus," and, although in NOD.c3c4 mice the pathology swings from the CBD to the intrahepatic biliary ducts as the disease progresses, in NOD and (NOD×NOD.c3c4)F1 mice the disease process is focused on the pancreas and pancreatic islets. Does a genetically controlled difference between these related strains modulate the early immune response in the gut, whether based on innate or adaptive immunity, to determine the anatomical "switchpoint" resulting in one syndrome or another? Because hyperresponsiveness of B cells to a Toll-like receptor stimulus has been shown in humans with PBC (21), the early B cell response in NOD.c3c4 mice is a priority in our laboratories. Notably, one of the handicaps to elucidating the nature of human autoimmune diseases is the protracted interval between actual disease onset and overt expression. The NOD.c3c4 and NOD.c3c4-*scid* strains now provide the opportunity to examine events at the very beginning of ABD. Moreover, the dissection of immunopathology of NOD. c3c4 mice will include a congenic mapping strategy to determine the precise genetic regions necessary and sufficient for the disease process, analogous to the genetic dissection ongoing in NOD mice (22). Comparison of the NOD.c3c4 with the genetically similar 1803 mouse demonstrates the sensitivity of the ABD process to quite minor changes in genetic make-up. A fundamental question is the causation of the "switch" from pancreatic islet to biliary tract in NOD and NOD.c3c4 mice, respectively, that are 95% genetically identical. The absence of ABD in strain 1803 suggests that the newly defined *Abd1* region, which is independent of any known *Idd* locus, interacts with *Idd* loci on chromosome 3 to generate a completely different autoimmune phenotype. Progressive reduction of the interval necessary for disease should reveal the identity of genes and their products that orchestrate the remarkable switch from diabetes to ABD.

MATERIALS AND METHODS

Animals, tissue, and sera. NOD.c3c4, NOD, NOD-*scid*, and B6.H2ᵍ⁷ (hereafter called B6.G7) mice were bred and housed under specific pathogen-free conditions, and all procedures were conducted according to approved protocols of the University of Pittsburgh School of Medicine Animal Care and Use Committee. NOD.B6/10 *Idd3/10/18*R323 *Idd9.1/9.2/9.3*R905 mice, hereafter designated strain 1803, were developed by intercrossing two established strains, NOD.B6 *Idd3/10/18*R323 and NOD.B10 *Idd9.1/9.2/ 9.3*R905, and genotyping multiple markers within each segment to establish a strain that is homozygous for both introgressed regions. Line 1803 was bred and housed at Taconic under specific pathogen-free conditions. Stored sera were used from NOD.B10*Idd9.1/9.2.9.3*R28 (previously designated NOD. c4a [reference 21] and called NOD.c4 here) and NOD.B6 *Idd3/10/18*R323

(previously designated NOD.c3a [reference 7] and called NOD.c3 here). The NOD.c4 strain and lines 1802 and 1803 are no longer extant. Strains NOD.c3c4, NOD.B6 *Idd3/10/18*R323, and NOD.B10 *Idd9*R905 are available as lines 1112, 1538, and 905 through the Emerging Models Program at Taconic. NOD.c3c4-*scid* mice were constructed as follows: NOD. 3c4 mice were mated to NOD-*scid* mice, and F1 mice were backcrossed to NOD.c3c4 mice. Progeny homozygous for the c3 and c4 intervals and heterozygous for the *scid* mutation were intercrossed. The *scid* homozygous intercross progeny were identified and became the founders of the NOD. c3c4-*scid* line. Sera and tissues were collected between the ages of 0 and 60, 60 and 100, 100 and 140, 140 and 200, and >200 d and stored at −80°C until use.

Liver histology. Liver tissues were immediately fixed in 10% buffered formalin, embedded in paraffin, and cut into 5-μm sections. Liver sections were deparaffinized, stained with hematoxylin and eosin, and evaluated microscopically for leukocytic infiltration. Eosinophils were defined by the presence of typical red granular cytoplasmic components in polynuclear cells. Immunohistochemical staining for CD3+ cells was performed using frozen tissues. In brief, liver sections were embedded in optimal cutting temperature compound (Tissue TEK) and frozen in liquid nitrogen. 5-μm-thick sections were cut with a cryostat, placed on 3-amino-propyltriethoxysilane–coated slides, and fixed in ice-cold acetone for 10 min. Slides were incubated in 0.3% H$_2$O$_2$, washed, and blocked with 10% goat serum in Protein Block (Immunon). The slides were then incubated with rat anti-CD3 1:100 (BD Biosciences) in a humidity chamber, washed with PBS, and incubated with biotinylated goat anti–rat (Jackson ImmunoResearch Laboratories). After washing, the slides were incubated with ABC (Vector Laboratories), washed, and incubated with AEC solution (Scytek). The slides were rinsed and counterstained with aqueous hematoxylin blue. CD4+, CD8+, and DC2 cells were detected by biotin-conjugated CD4 (L3T4, clone RM4-5; eBioscience), CD8a (Ly-2, clone 53–6.7; eBioscience), and pDCA1 (clone JF05-1C24.1; Miltenyi Biotec), respectively. After washing, the slides were incubated with ABC (Vector Laboratories), washed, incubated with diaminobenzidine (DakoCytomation), and counterstained with hematoxylin blue. Known positive and negative samples were incubated throughout, and optimal dilutions of primary and secondary antibodies were used.

Preparation of splenocytes and HLCs. The spleen from each mouse was removed aseptically, and a single cell suspension was prepared. After lysing RBCs, the splenocytes were washed three times with PBS. HLCs were collected after liver perfusion using Percoll density gradient centrifugation as described previously (23, 24). In brief, the liver was perfused postmortem with PBS via the portal vein, cut into small pieces, and pressed through wire mesh. After being washed with PBS, the cells were resuspended in 35% Percoll solution (GE Healthcare) and centrifuged at 1,500 rpm for 30 min at room temperature. The pellet was resuspended in lysis solution to remove RBCs and washed twice in medium.

Cell purification and stimulation. CD4+ or CD8+ cells were prepared by magnetic separation using a MiniMACS system (Miltenyi Biotec; reference 25). In brief, splenocytes were incubated with anti-CD4 or anti-CD8 magnetic microbeads for 15 min, washed, and collected on a magnetic flow-through column. Purified cells were stimulated as described previously (25). In brief, cells were suspended in complete medium consisting of RPMI 1640 supplemented with 10% (wt/vol) FCS, 1 mM L-alanyl-glutamine (Life Technologies), 100 U/ml penicillin, 100 μg/ml streptomycin (Life Technologies), 1 mM sodium pyruvate (Life Technologies), and 50 μM 2-ME. Cells were then transferred to 24-well plates precoated with anti-CD3 antibody, and 1 μg/ml anti-CD28 antibody (BD Biosciences) was added to each well. The cells were cultured for 72 h at 37°C in a humidified 5% CO$_2$ atmosphere. The supernatants were collected at the end of culture and stored at −80°C.

Cytokine measurement by ELISA. Cytokines (IFN-γ, IL-4, and IL-2) were measured by ELISA as described previously (25). In brief, a flat-bottom 96-well plate was coated with anti–IFN-γ, anti–IL-4, or anti–IL-2 antibodies

(BD Biosciences) at 4°C overnight. Cell culture supernatants were added, and the plate was incubated for 2 h. After washing, the plate was incubated with biotinylated anti–IFN-γ, anti–IL-4, or anti–IL-2 antibodies (BD Biosciences) for 1 h, and then washed and incubated for 1 h with europium-avidin solution (PerkinElmer). Enhancement solution (PerkinElmer) was added, and the europium fluorescence was measured with a Victor 1420 ELISA reader.

RNase protection assay. Total RNA was extracted from cultured cells using the RNeasy mini kit (QIAGEN). The RNA was re-dissolved in RNase-free water, and the yield was estimated by spectrophotometry. Equal quantities of RNA were used for analysis. RNase protection assay was performed using RiboQuant (BD Biosciences) according to the manufacturer's protocol. Multiprobe template set mCK-1 (containing templates for IL-4, IL-5, IL-10, IL-13, IL-15, IL-9, IL-2, IL-6, IF-, L32, and GAPDH) was purchased from BD Biosciences. The templates were used to synthesize the [-32P]UTP-labeled probes (3,000 Ci/mmol, 10 mCi/ml; NEN Life Science Products) in the presence of a GACU pool using a T7 RNA polymerase (BD Biosciences). Hybridization with 5–15 μg RNA was performed for 12–14 h at 56°C, and the products were digested with an RNase A and T1 mixture. The samples were treated by proteinase K in proteinase K buffer with yeast tRNA, extracted with phenol and chloroform/isoamyl alcohol (50:1), and precipitated in the presence of ammonium acetate. The samples were loaded on an acrylamide-urea gel and run at 40 W with 0.5× Tris-borate/EDTA electrophoresis buffer for 2 h. The gel was adsorbed to filter paper, vacuum dried, and exposed on film (X-AR; Kodak) with intensifying screens at −70°C.

In vivo treatment with anti-CD3 antibody. 6–10-wk-old NOD.c3c4 mice were treated with a single dose of 200 μg anti-CD3 antibody (145-2C11), and control mice were treated with PBS alone. Mice were analyzed for disease and disease-related phenotypes ∼3 mo after treatment.

Flow cytometry. Antibodies against CD4, CD8, CD19, CD122, γδ TCR, CD69, T cell β receptor, and Gr-1 were purchased from BD Biosciences. Cells were incubated with Fc blocker (BD Biosciences) and stained with saturating levels of labeled antibodies for 20 min at 4°C. Samples were analyzed on a FACSCalibur (Becton Dickinson).

Immunoreactivity to mitochondria and epitope specificity analysis. Immunoreactivity of serum samples to the major mitochondrial antigen, PDC-E2, was studied by immunoblotting as described previously (26). In brief, 20 μg recombinant protein was resolved by SDS-PAGE, transferred onto nitrocellulose membranes, blocked with 3% nonfat dry milk in PBS, and probed with sera from NOD.c3c4 and control mice (1:200 dilution) for 1 h. After three 5-min washes with PBS/0.05% Tween-20, the membranes were incubated with horseradish peroxidase–conjugated anti–mouse IgG (Zymed Laboratories), washed with PBS/0.05% Tween-20, and developed by chemiluminescence. Known positive mAb to PDC-E2 (27) was used as a positive control. To determine the specific PDC-E2 epitope recognized, recombinant PDC-E2 outer lipoyl domain, inner lipoyl domain, E1/E3 binding site, and the catalytic domain were resolved on 10% SDS-PAGE, transferred to nitrocellulose membranes, and probed with AMA+ serum samples and developed as described above.

PDC enzyme inhibition assay. To determine if NOD.c3c4 sera inhibit PDC enzyme activity, sera (1:100) from 7-mo-old NOD.c3c4 mice were incubated with purified PDC (Sigma-Aldrich) for 10 min at room temperature and added to a mixture containing 5 mM sodium pyruvate, 2.5 mM NAD+, 0.2 mM thiamine pyrophosphate, 0.1 mM coenzyme A, 0.3 mM dithiothreitol, 1 mM magnesium chloride, and 50 mM potassium phosphate buffer, pH 8.0. Changes in absorbency per minute at 340 nm were monitored for 5 min. Inhibition of PDC enzyme activity by serum samples from control NOD mice, human PBC patients, and healthy human control human sera were analyzed in parallel using 6 sera/group. Enzyme activity

without sera was determined in parallel, and the values were defined as 100% activity.

REFERENCES

1. Gershwin, M.E., A.A. Ansari, I.R. Mackay, Y. Nakanuma, A. Nishio, M.J. Rowley, and R.L. Coppel. 2000. Primary biliary cirrhosis: an orchestrated immune response against epithelial cells. *Immunol. Rev.* 174:210–225.

2. Coppel, R.L., L.J. McNeilage, C.D. Surh, J. Van de Water, T.W. Spithill, S. Whittingham, and M.E. Gershwin. 1988. Primary structure of the human M2 mitochondrial autoantigen of primary biliary cirrhosis: dihydrolipoamide acetyltransferase. *Proc. Natl. Acad. Sci. USA.* 85:7317–7321.

3. Gershwin, M.E., I.R. Mackay, A. Sturgess, and R.L. Coppel. 1987. Identification and specificity of a cDNA encoding the 70 kd mitochondrial antigen recognized in primary biliary cirrhosis. *J. Immunol.* 138:3525–3531.

4. Van de Water, J., M.E. Gershwin, P. Leung, A. Ansari, and R.L. Coppel. 1988. The autoepitope of the 74-kD mitochondrial autoantigen of primary biliary cirrhosis corresponds to the functional site of dihydrolipoamide acetyltransferase. *J. Exp. Med.* 167:1791–1799.

5. Van de Water, J., A.A. Ansari, C.D. Surh, R. Coppel, T. Roche, H. Bonkovsky, M. Kaplan, and M.E. Gershwin. 1991. Evidence for the targeting by 2-oxo-dehydrogenase enzymes in the T cell response of primary biliary cirrhosis. *J. Immunol.* 146:89–94.

6. Jones, D.E., J.M. Palmer, O.F. James, S.J. Yeaman, M.F. Bassendine, and A.G. Diamond. 1995. T-cell responses to the components of pyruvate dehydrogenase complex in primary biliary cirrhosis. *Hepatology.* 21:995–1002.

7. Koarada, S., Y. Wu, N. Fertig, D.A. Sass, M. Nalesnik, J.A. Todd, P.A. Lyons, J. Fenyk-Melody, D.B. Rainbow, L.S. Wicker, et al. 2004. Genetic control of autoimmunity: protection from diabetes, but spontaneous autoimmune biliary disease in a nonobese diabetic congenic strain. *J. Immunol.* 173:2315–2323.

8. Bach, J.F., and D. Mathis. 1997. The NOD mouse. *Res. Immunol.* 148:285–286.

9. Rasooly, L., C.L. Burek, and N.R. Rose. 1996. Iodine-induced autoimmune thyroiditis in NOD-H-2h4 mice. *Clin. Immunol. Immunopathol.* 81:287–292.

10. Cha, S., H. Nagashima, V.B. Brown, A.B. Peck, and M.G. Humphreys-Beher. 2002. Two NOD Idd-associated intervals contribute synergistically to the development of autoimmune exocrinopathy (Sjogren's syndrome) on a healthy murine background. *Arthritis Rheum.* 46:1390–1398.

11. Matsumoto, I., A. Staub, C. Benoist, and D. Mathis. 1999. Arthritis provoked by linked T and B cell recognition of a glycolytic enzyme. *Science.* 286:1732–1735.

12. Tobe, K., T. Itoshima, T. Tsuchiya, R. Fujiwara, G. Yamada, H. Nagashima, and T. Kobayashi. 1985. Electron microscopy of granulomatous lesions of the liver in primary biliary cirrhosis. *Acta Pathol. Jpn.* 35:1309–1318.

13. Terasaki, S., Y. Nakanuma, M. Yamazaki, and M. Unoura. 1993. Eosinophilic infiltration of the liver in primary biliary cirrhosis: a morphological study. *Hepatology.* 17:206–212.

14. Goldstein, N.S., A. Soman, and S.C. Gordon. 2001. Portal tract eosinophils and hepatocyte cytokeratin 7 immunoreactivity helps distinguish early-stage, mildly active primary biliary cirrhosis and autoimmune hepatitis. *Am. J. Clin. Pathol.* 116:846–853.

15. Chatenoud, L., E. Thervet, J. Primo, and J.F. Bach. 1994. Anti-CD3 antibody induces long-term remission of overt autoimmunity in nonobese diabetic mice. *Proc. Natl. Acad. Sci. USA.* 91:123–127.

16. Wu, C.T., J.P. Eiserich, A.A. Ansari, R.L. Coppel, S. Balasubramanian, C.L. Bowlus, M.E. Gershwin, and J. Van De Water. 2003. Myeloperoxidase-positive inflammatory cells participate in bile duct damage in primary biliary cirrhosis through nitric oxide–mediated reactions. *Hepatology.* 38:1018–1025.

17. Kita, H., Z.X. Lian, J. Van de Water, X.S. He, S. Matsumura, M. Kaplan, V. Luketic, R.L. Coppel, A.A. Ansari, and M.E. Gershwin. 2002. Identification of HLA-A2–restricted CD8^{+} cytotoxic T cell responses in primary biliary cirrhosis: T cell activation is augmented by immune complexes cross-presented by dendritic cells. *J. Exp. Med.* 195:113–123.

18. Kita, H., S. Matsumura, X.S. He, A.A. Ansari, Z.X. Lian, J. Van de Water, R.L. Coppel, M.M. Kaplan, and M.E. Gershwin. 2002. Quantitative and functional analysis of PDC-E2-specific autoreactive cytotoxic T lymphocytes in primary biliary cirrhosis. *J. Clin. Invest.* 109:1231–1240.

19. Krams, S.M., C.D. Surh, R.L. Coppel, A. Ansari, B. Ruebner, and M.E. Gershwin. 1989. Immunization of experimental animals with dihydrolipoamide acetyltransferase, as a purified recombinant polypeptide, generates mitochondrial antibodies but not primary biliary cirrhosis. *Hepatology.* 9:411–416.

20. Eisenberg, R.A., S.Y. Craven, R.W. Warren, and P.L. Cohen. 1987. Stochastic control of anti-Sm autoantibodies in MRL/Mp-lpr/lpr mice. *J. Clin. Invest.* 80:691–697.

21. Kikuchi, K., Z.X. Lian, G.X. Yang, A.A. Ansari, S. Ikehara, M. Kaplan, H. Miyakawa, R.L. Coppel, and M.E. Gershwin. 2005. Bacterial CpG induces hyper-IgM production in CD27(+) memory B cells in primary biliary cirrhosis. *Gastroenterology.* 128:304–312.

22. Wicker, L.S., J.A. Todd, and L.B. Peterson. 1995. Genetic control of autoimmune diabetes in the NOD mouse. *Annu. Rev. Immunol.* 13:179–200.

23. Huang, L., G. Soldevila, M. Leeker, R. Flavell, and I.N. Crispe. 1994. The liver eliminates T cells undergoing antigen-triggered apoptosis in vivo. *Immunity.* 1:741–749.

24. Yamamoto, S., Y. Sato, T. Shimizu, R.C. Halder, H. Oya, M. Bannai, K. Suzuki, H. Ishikawa, K. Hatakeyama, and T. Abo. 1999. Consistent infiltration of thymus-derived T cells into the parenchymal space of the liver in normal mice. *Hepatology.* 30:705–713.

25. Koarada, S., Y. Wu, G. Olshansky, and W.M. Ridgway. 2002. Increased nonobese diabetic Th1:Th2 (IFN-gamma:IL-4) ratio is CD4+ T cell intrinsic and independent of APC genetic background. *J. Immunol.* 169:6580–6587.

26. Leung, P.S., C. Quan, O. Park, J. Van de Water, M.J. Kurth, M.H. Nantz, A.A. Ansari, R.L. Coppel, K.S. Lam, and M.E. Gershwin. 2003. Immunization with a xenobiotic 6-bromohexanoate bovine serum albumin conjugate induces antimitochondrial antibodies. *J. Immunol.* 170:5326–5332.

27. Migliaccio, C., A. Nishio, J. Van de Water, A.A. Ansari, P.S. Leung, Y. Nakanuma, R.L. Coppel, and M.E. Gershwin. 1998. Monoclonal antibodies to mitochondrial E2 components define autoepitopes in primary biliary cirrhosis. *J. Immunol.* 161:5157–5163.